Ⓔ

A Database of Shear-Wave Splitting Measurements for the Arabian Plate

by Saleh Qaysi, Kelly H. Liu, and Stephen S. Gao

ABSTRACT

We present a uniform database of teleseismic shear-wave splitting (SWS) parameters for the Arabian plate. The SWS parameters, including the fast polarization orientation and splitting time, are measured based on a procedure that minimizes the energy on the transverse component. The majority of the data used to produce the SWS database were recorded by 157 seismic stations operated by the Saudi Geological Survey from 2010 to 2015. The rest of the data from 25 stations were obtained from the Incorporated Research Institutions for Seismology (IRIS) Data Management Center (DMC). About 4000 pairs of well-defined SKS, SKKS, and PKS parameters were obtained. Most of the stations show dominantly north–south (N-S) fast orientations. The station-averaged splitting times range from 0.45 to 1.84 s, with large splitting times in the western region of the Arabian Peninsula, and decrease eastward. The newly established database has an unprecedented spatial coverage and can be utilized by researchers in various fields to investigate crustal and mantle structure and dynamics beneath the Arabian plate.

Electronic Supplement: Tables of individual shear-wave splitting measurements, station-averaged splitting parameters, and area-averaged splitting parameters.

INTRODUCTION

Over the past several decades, shear-wave splitting (SWS) analysis has been increasingly utilized to study seismic anisotropy in the lithosphere and asthenosphere (Hess, 1964; Silver and Chan, 1991; Silver, 1996; Savage, 1999; Fouch and Rondenay, 2006; Long and Becker, 2010; Liu *et al.*, 2014; Yang *et al.*, 2017). When a shear wave generated by *P*-to-*S* conversion at the core-mantle boundary propagates into an anisotropic medium along its ray path, it splits into fast and slow components traveling at different speeds. The SWS parameters are the polarization orientation of the fast component and the time delay between the fast and slow components (Vinnik *et al.*, 1989; Silver and Chan, 1991; Savage, 1999; Liu and Gao, 2013). Numerous experimental and observational studies indicate that in the mantle, SWS is primarily caused by azimuthal anisotropy related to the lattice preferred orientation of olivine, which consists of more than 65% of the Earth's upper mantle (McKenzie, 1979; Silver and Chan, 1991; Jung and Karato, 2001; Conrad *et al.*, 2007). In a uniaxial compressional system, the a axis of olivine becomes perpendicular to the maximum compressional strain. It becomes parallel to the flow direction in a simple shear regime (Zhang and Karato, 1995; Silver *et al.*, 2001). The shear wave splits twice if it enters two layers of anisotropy with different orientations and the apparent splitting parameters vary as a function of the arriving azimuth of the shear wave (i.e., back azimuth [BAZ]) with a $\pi/2$ periodicity (Silver and Savage, 1994; Yang *et al.*, 2016).

Several SWS studies in the Arabian plate and adjacent regions have been conducted. Using SKS data from eight portable seismic stations deployed across the Arabian shield from November 1995 to March 1997, Wolfe *et al.* (1999) observed mostly north–south (N-S) fast orientations. The observed seismic anisotropy was interpreted as fossil anisotropy associated with the dominantly east–west (E-W) accretion of oceanic terranes of the Proterozoic Arabia. Mantle anisotropy was also studied along the Red Sea and the Arabian Peninsula using SKS data recorded at 35 broadband stations from three different seismic networks (Hansen *et al.*, 2006). The results indicated that the majority of the fast orientations in the Arabian plate are N-S. The SWS measurements near the Gulf of Aqaba show a fast orientation that is parallel to the Dead Sea fault, probably due to the strike-slip motion between the African and the Arabian plates. Using data obtained from 47 seismic stations deployed on both sides of the Red Sea, Elsheikh *et al.* (2014) obtained about 1100 pairs of individual SKS, SKKS, and PKS splitting parameters to investigate mantle dynamics and anisotropy forming mechanisms. N-S fast orientations were observed at almost all of the stations and are inconsistent with the strike of major tectonic boundaries, indicating that the observed anisotropy is developed in the transitional layer between the partially coupled lithosphere and asthenosphere rather than purely lithospheric (Elsheikh *et al.*, 2014).

Over the past several years, we have developed a procedure to systematically measure and rank and manually check the individual SWS parameters, and have used the procedure to

(a)

(b)
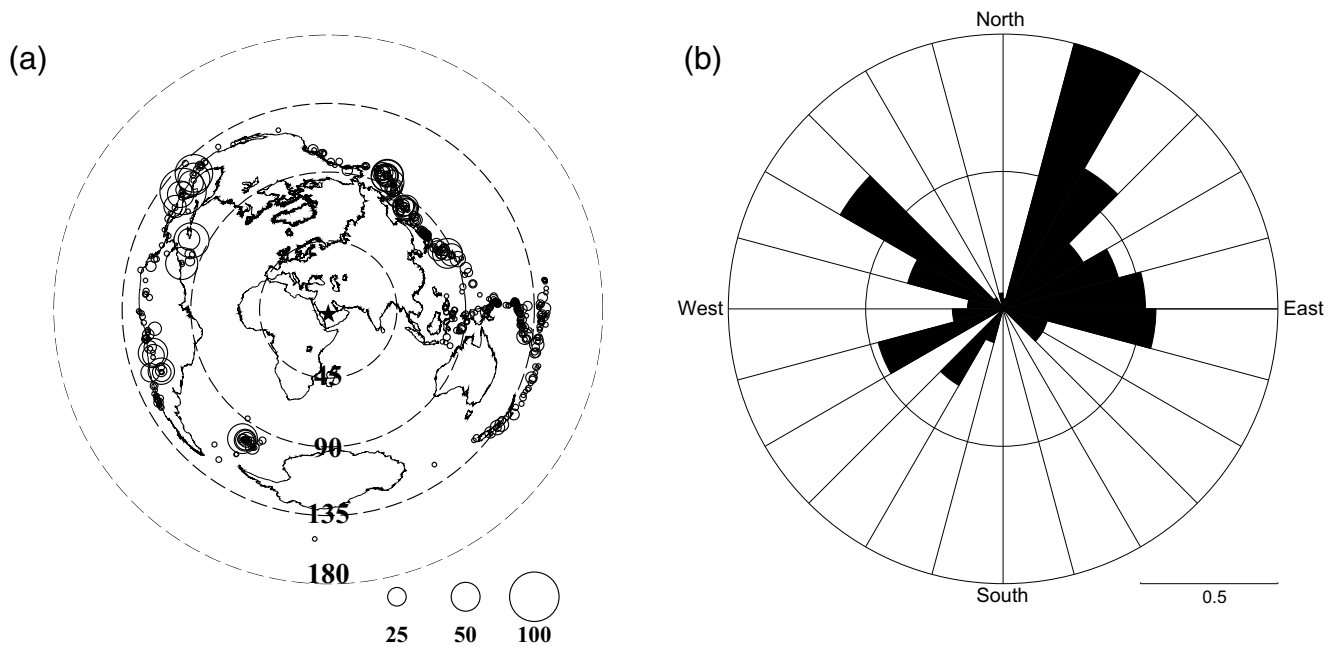
▲ **Figure 1.** (a) Distribution of earthquakes used in the study. The sizes of the circles are related to the number of qualities A and B shear-wave splitting (SWS) parameters. (b) Distribution of the back azimuth of the events. The star represents the center of the study area.

produce a uniform SWS parameter database for the contiguous United States (Liu, 2009; Liu et al., 2014; Yang et al., 2016, 2017). Here, we present a uniform SWS database for the Arabian plate using the same procedure by taking the advantage of the recent availability of data from about 200 stations.

DATA AND METHOD

The three-component broadband seismic data utilized in the study were recorded at 157 stations operated by the Saudi Geological Survey (SGS) under the National Center of Earthquakes and Volcanoes, Saudi Arabia. In addition, data from 25 stations were acquired from the Incorporated Research Institutions for Seismology (IRIS) Data Management Center (DMC). The recording duration was from January 2010 to June 2015 for the SGS stations and from August 1994 to August 2017 for the IRIS stations.

The data processing and result ranking procedures used in the study are identical to those described in Liu and Gao (2013), and are briefly summarized here. We utilize the P-to-S converted phases at the core-mantle boundary, including PKS, SKKS, and SKS (collectively called XKS) to obtain the splitting parameters. To ensure that all the possible XKS (including the core-diffracted components) are included, the epicentral distance for data requesting is 120°–180°, 95°–180°, and 84°–180°, respectively. The cutoff
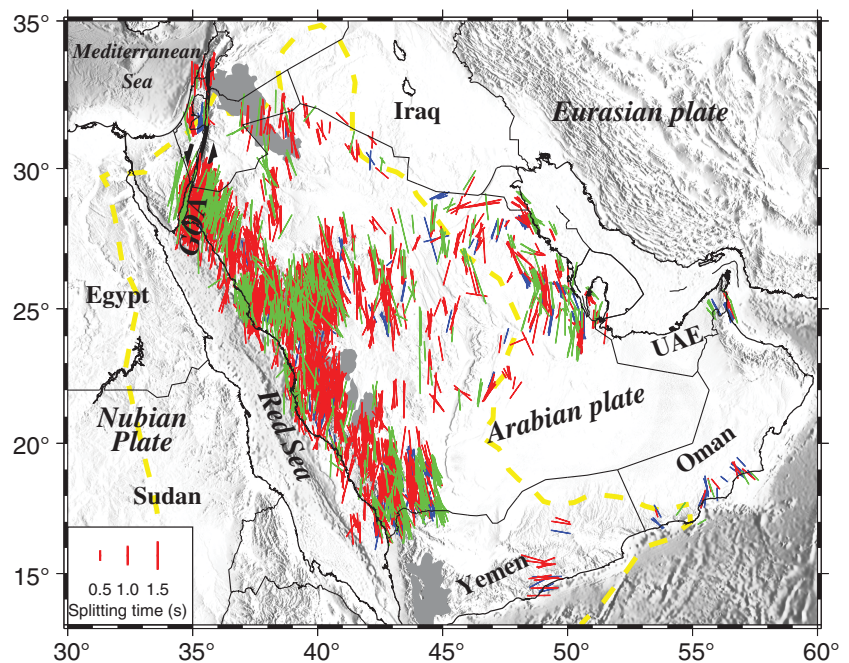
▲ **Figure 2.** Topographic map of the Arabian plate showing the individual SWS measurements from PKS (blue bar), SKKS (green bar), and SKS (red bar) plotted above the 200 km depth ray-piercing points. The dashed yellow line indicates the Afro-Arabian dome. GOA, Gulf of Aqaba.

magnitude is 5.6, which is reduced to 5.5 for earthquakes with a focal depth greater than 100 km. A total of 491 events contributed to one or more measurements (Fig. 1). The seismograms are detrended and filtered with a 0.04–0.5 Hz

frequency band. The initial time window used for computing the SWS parameters begins at 5 s before and ends at 20 s after the theoretical arrival of the XKS phase, and is adjusted, if necessary, during the manual checking stage (Liu, 2009; Liu *et al.*, 2014).

The technique used to calculate the SWS parameters is based on the minimization of the energy on the transverse component approach (Silver and Chan, 1991), which has been found to be the most reliable for noisy data (Vecsey *et al.*, 2008). The SWS measurements are ranked on the basis of the combination of signal-to-noise ratio (SNR) on the original and corrected radial and transverse components. The specific SNR values can be found in Liu *et al.* (2008). The measurements are initially ranked automatically as qualities A (outstanding), B (good), C (poor), or N (null) (Liu *et al.*, 2008), followed by manual checking to ensure quality. The manual checking includes adjusting the XKS window, tuning the filtering frequencies, and verifying the quality ranking if necessary (Liu and Gao, 2013). Only qualities A and B measurements are included in the database.

DATABASE CONTENTS

After manual checking, a total of 3998 pairs of individual splitting parameters are ranked as either quality A or quality B, among which 428, 665, and 2905 are from the PKS, SKKS, and SKS phases, respectively (Fig. 2). Similar to the SWS databases that we produced for the United States (Liu *et al.*, 2014; Yang *et al.*, 2016), the final database includes the individual SWS parameters (Fig. 2; Ⓔ Table S1, available in the electronic supplement to this article), station-averaged parameters (Fig. 3; Ⓔ Table S2), and area-averaged parameters (Fig. 4; Ⓔ Table S3). The averaged fast orientations are calculated as the circular mean of the measured fast orientations (Mardia and Jupp, 2000), whereas the averaged splitting times are arithmetic means.

The individual SWS parameter database (Ⓔ Table S1) has 17 columns, which are identical to the database that we produced for North America (Liu *et al.*, 2014; Yang *et al.*, 2016), including the station name, phase name, event name, station latitude, station longitude, fast orientation, standard deviation of the fast orientation, splitting time, standard deviation of the splitting time, BAZ, modulo-90° of the BAZ, event latitude, event longitude, focal depth, rank of the measurements, and the latitude and longitude of the ray-piercing points at 200 km depth.
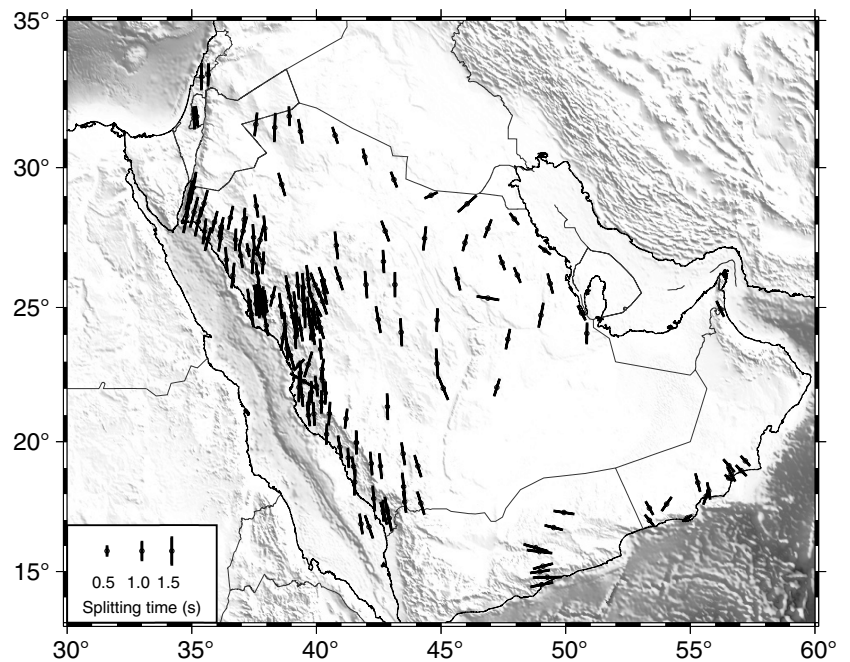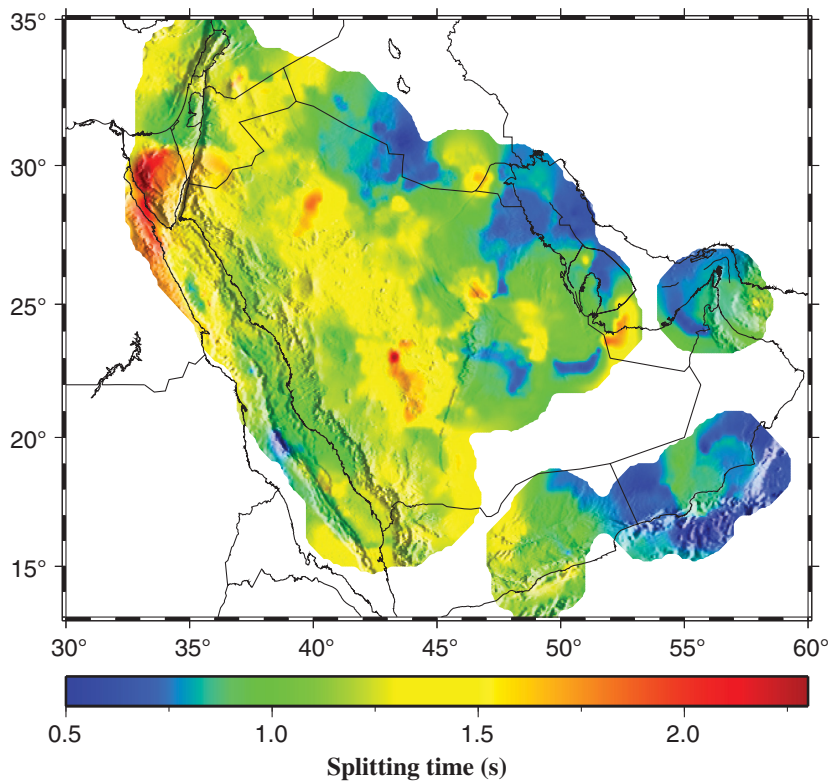

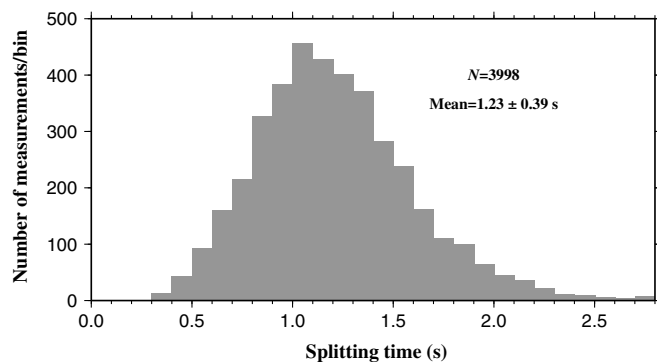▲ **Figure 3.** Station-averaged SWS parameters.
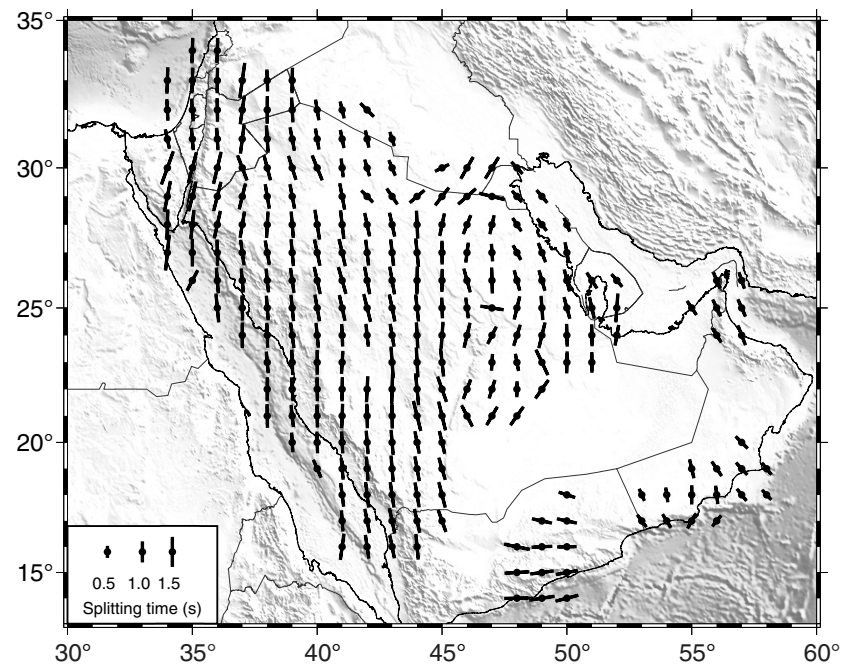
▲ **Figure 4.** Area-averaged SWS parameters in radius = 1° circles at 200 km depth.

The database for the station-averaged SWS parameters (Ⓔ Table S2) has eight columns (Liu *et al.*, 2014; Yang *et al.*, 2016) including the name, latitude, and longitude of the station, mean fast orientation, standard deviation of the mean fast orientation, mean splitting time, standard deviation of the mean splitting time, and the number of splitting measurements participated in calculating the station averages.

▲ **Figure 5.** Distribution of spatially averaged splitting times in radius = 1° circles.
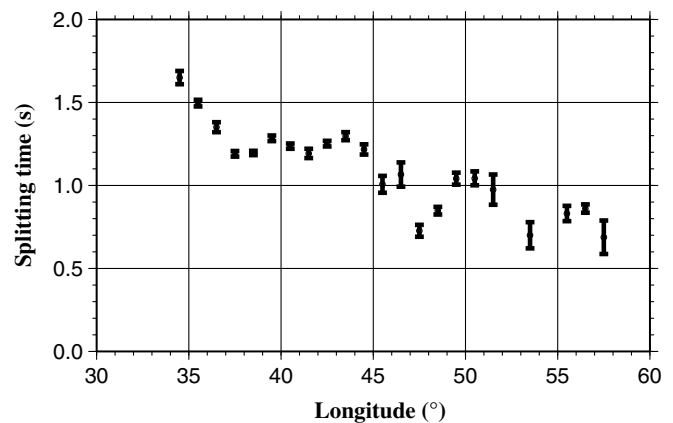
SPATIAL AND AZIMUTHAL VARIATIONS OF THE OBSERVED SHEAR-WAVE SPLITTING PARAMETERS

The majority of the stations show N-S fast orientations beneath the Arabian plate, except for the mostly E-W measurements in Yemen (Figs. 2 and 3). Careful visual checking of the azimuthal variation of splitting parameters indicates that no systematic variation of the parameters with the BAZ is observed for the majority of the stations in the study area. Therefore, a model with a single anisotropic layer and a horizontal axis of symmetry is sufficient to explain the observed SWS parameters.

The spatial distribution of the averaged splitting times is calculated based on the mean value of individual splitting times in radius = 1° circular bins with a moving interval of 0.25°. Large splitting times up to about 2.5 s are observed on the Afro-Arabian dome (Arabian shield; Fig. 5), and small splitting times as low as 0.4 s are mostly observed near the eastern edge of the plate, where the majority of the stations are characterized by splitting times in the 0.5–1.0 s range (Figs. 6 and 7). The splitting times decrease systematically from the Arabian shield to the eastern margin of the study area (Fig. 7).

CONCLUSIONS

We produced a uniform database of individual SWS parameters using data from 182 stations in the Arabian plate. The database contains well-defined individual, station-averaged, and area-averaged SWS measurements. The database has a potential to be used by investigators in various fields to study

To produce area-averaged SWS parameters (Fig. 4 and Ⓔ Table S3), the SWS individual parameters are grouped into 1° circular bins based on the location of the piercing points at 200 km depth, and those in the same bin are averaged. The area-averaged dataset (Ⓔ Table S3) has seven columns (Liu et al., 2014), which include the latitude and the longitude of the center of the bin, mean fast orientation, standard deviation of the mean fast orientation, mean splitting time, standard deviation of the mean splitting time, and the number of splitting measurements in the bin.

▲ **Figure 6.** Histogram showing the distribution of XKS splitting times in the study area.

▲ **Figure 7.** Splitting times averaged over longitudinal bands of 1° wide. A systematic eastward decrease is observed.

the structure and dynamics of the Earth's interior, from the crust to the core-mantle boundary beneath the Arabian plate.

DATA AND RESOURCES

ACKNOWLEDGMENTS

REFERENCES

Conrad, C. P., M. D. Behn, and P. G. Silver (2007). Global mantle flow and the development of seismic anisotropy: Differences between the oceanic and continental upper mantle, *J. Geophy. Res.* **112,** no. B07317, doi: 10.1029/2006JB004608.

Elsheikh, A. A., S. S. Gao, K. H. Liu, A. A. Mohamed, Y. Yu, and R. E. Fat-Helbary (2014). Seismic anisotropy and subduction-induced mantle fabrics beneath the Arabian and Nubian plates adjacent to the Red Sea, *Geophys. Res. Lett.* **41,** 2376–2381, doi: 10.1002/2014GL059536.

Fouch, M. J., and S. Rondenay (2006). Seismic anisotropy beneath stable continental interiors, *Phys. Earth Planet. In.* **158,** 292–320.

Hansen, S., S. Schwartz, A. Al-Amri, and A. Rodgers (2006). Combined plate motion and density-driven flow in the asthenosphere beneath Saudi Arabia: Evidence from shear-wave splitting and seismic anisotropy, *Geology* 34**,** 869–872, doi: 10.1130/G22713.1.

Hess, H. H. (1964). Seismic anisotropy of the uppermost mantle under oceans, *Nature* **203,** 629–631.

Jung, H., and S. I. Karato (2001). Water-induced fabric transitions in olivine, *Science* **293,** 1460–1463.

Liu, K. H. (2009). NA-SWS-1.1: A uniform database of teleseismic shear wave splitting measurements for North America, *Geochem. Geophys. Geosys.* **10,** no. Q05011, doi: 10.1029/2009GC002440.

Liu, K. H., and S. S. Gao (2013). Making reliable shear-wave splitting measurements, *Bull. Seismol. Soc. Am.* **103,** no. 5, 2680–2693, doi: 10.1785/0120120355.

Liu, K. H., A. Elsheikh, A. Lemnifi, U. Purevsuren, M. Ray, H. Refayee, B. Yang, Y. Yu, and S. S. Gao (2014). A uniform database of teleseismic shear wave splitting measurements for the western and central United States, *Geochem. Geophys. Geosys.* **15,** 2075–2085, doi: 10.1002/2014GC005267.

Liu, K. H., S. S. Gao, Y. Gao, and J. Wu (2008). Shear wave splitting and mantle flow associated with the deflected Pacific slab beneath northeast Asia, *J. Geophys. Res.* **113,** no. B01305, doi: 10.1029/2007JB005178.

Long, M. D., and T. W. Becker (2010). Mantle dynamics and seismic anisotropy, *Earth Planet. Sci. Lett.* **297,** 341–354.

Mardia, K. V., and P. Jupp (2000). *Directional Statistics*, Second Ed., John Wiley and Sons Ltd., Chichester, United Kingdom.

McKenzie, D. (1979). Finite deformation during fluid flow, *Geophys. J. Int.* **58,** 689–715.

Savage, M. K. (1999). Seismic anisotropy and mantle deformation: What have we learned from shear wave splitting?, *Rev. Geophys.* **37,** 65–106.

Silver, P. G. (1996). Seismic anisotropy beneath the continents: Probing the depths of geology, *Ann. Rev. Earth Planet. Sci.* **24,** 385–432.

Silver, P. G., and W. W. Chan (1991). Shear wave splitting and subcontinental mantle deformation, *J. Geophys. Res.* **96,** no. B10, 16,429–16,454.

Silver, P. G., and M. K. Savage (1994). The interpretation of shear-wave splitting parameters in the presence of two anisotropic layers, *Geophys. J. Int.* **119,** no. 3, 949–963.

Silver, P. G., S. S. Gao, K. H. Liu, and , and the Kaapvaal Seismic Group (2001). Mantle deformation beneath southern Africa, *Geophys. Res. Lett.* **28,** 2493–2496.

Vecsey, L., J. Plomerova, and V. Babuska (2008). Shear-wave splitting measurements: Problems and solutions, *Tectonophysics* **426,** 178–196.

Vinnik, L. P., V. Farra, and B. Romanowicz (1989). Azimuthal anisotropy in the Earth from observations of SKS at Geoscope and NARS broadband stations, *Bull. Seismol. Soc. Am.* **79,** no. 5, 1542–1558.

Wolfe, C. J., F. L. Vernon III, and A. Al-Amri (1999). Shear-wave splitting across western Saudi Arabia: The pattern of upper mantle anisotropy at a Proterozoic shield, *Geophys. Res. Lett.* **26,** no. 6, 779–782.

Yang, B. B., K. H. Liu, H. H. Dahm, and S. S. Gao (2016). A uniform database of teleseismic shear-wave splitting measurements for the western and central United States: December 2014 update, *Seismol. Res. Lett.* **87,** no. 2A, 295–300, doi: 10.1785/0220150213.

Yang, B. B., Y. Liu, H. Dahm, K. H. Liu, and S. S. Gao (2017). Seismic azimuthal anisotropy beneath the eastern United States and its geodynamic implications, *Geophys. Res. Lett.* **44,** no. 6, 2670–2678, doi: 10.1002/2016GL071227.

Zhang, S., and S. Karato (1995). Lattice preferred orientation of olivine aggregates deformed in simple shear, *Nature* **375,** 774–777.

Saleh Qaysi[1]
Kelly H. Liu
Stephen S. Gao
Geology and Geophysics Program
Missouri University of Science and Technology
Rolla, Missouri 65409 U.S.A.
liukh@mst.edu

[1] Also at Department of Geology and Geophysics, King Saud University, Riyadh 11451, Saudi Arabia.